THE BELL SYSTEM TECHNICAL JOURNAL
Vol. 56, No. 5, May–June 1977
Printed in U.S.A.

Dual-Polarized Channel Outages During Multipath Fading

By T. O. MOTTL

(Manuscript received December 8, 1976)

A statistical model for outages that occur in a dual-polarized-frequency radio channel during periods of multipath fading is proposed, and an analytical expression for outage time obtained. The model, which results in Rice-Nakagami statistics for the cochannel interference signal, describes channel outage time as a function of several environmental and radio-system parameters. The formulation obtained allows for efficient parameteric studies to evaluate the importance of these parameters to channel outage time and to examine parameter sensitivity questions. Results of practical significance relative to hardware XPD requirements, maximum hop length, system gain, dependence on geographic environment, and digital terminal performance characteristics are obtained for present 11-GHz QCPSK (quaternary-coherent-phase-shift-keyed) digital radio systems. Estimates of dual-polarized-frequency channel outage time are obtained for a variety of representative system parameter values and compared with expected outage times for a conventional channel. Particular attention is given to the mechanism of channel outages during multipath fading, and several potential means for control and/or reduction of channel outage time are discussed.

I. INTRODUCTION

1.1 DPF radio systems

Federal regulatory requirements for the channel capacity of an 11-GHz digital radio system are achieved in some short-haul radio systems by a diplex approach that uses each available radio-channel frequency band twice. Such designs, denoted here as dual-polarized-frequency (DPF) radio systems, are based on the high isolation theoretically obtainable between the two linear polarizations (vertical and horizontal) available for propagation at each radio-wave frequency.

Practical implementation of a DPF radio system relies on the attainability of high polarization isolation in the radio system, in the antenna system, and over the propagation path, and on the maintainability of these conditions. At any given frequency, degradation in the isolation between the orthogonally polarized signals can result in cochannel interference, with attendant degradation in the channel bit-error rate (BER).

This paper presents a theoretical modeling study of DPF radio channel reliability during periods of multipath fading. Using channel bit-error rate as a criterion, the effects of the polarization-isolation properties of system hardware and the propagation path on channel-outage time are evaluated. The sensitivity of bit-error rate to system hardware and propagation-path characteristics is of particular interest because of their direct impact on feasibility and cost of DPF radio systems.

A complete listing of all symbols and notation used in this paper is provided in Appendix A.

1.2 Linear polarization isolation

During periods of multipath fading activity, measurements on 11-GHz radio waves propagated along line-of-sight paths display statistical fluctuations in the isolation between orthogonal linearly polarized waves at the same frequency.[1–4] A convenient measure of the isolation between two cross-polarized signals—i.e., signals transmitted via such orthogonally polarized waves—is the cross-polarization-discrimination ratio or XPD. The XPD is defined as the ratio (usually expressed in dB) of the energy received on a reference polarization that results from a signal transmitted with the same polarization (the copolarized, desired signal) to the energy received on this same polarization but transmitted with the orthogonal polarization (the cross-polarized or interference signal).

1.3 Multipath outage estimates

Estimates of single-hop (point-to-point) outage probabilities for 11-GHz QCPSK digital radio systems were first obtained by Lin in 1973 based in part on a one-parameter model for the RMS-XPD ratio during multipath fading. In this model, at any fixed fade depth in the deep-fade region, the cross-polarized voltage envelope varies as a Rayleigh distributed random variable, and the RMS-XPD behaves as a linear function of the fade depth in dB, as shown by curve "L" in Fig. 1.

Some early experimental data[4] showed a nonlinear dependence of RMS-XPD vs fade depth, with linear proportionality between RMS-XPD and fade depth only during deep multipath fading, e.g., fades greater than 10 to 15 dB. Curve NL in Fig. 1 is a plot of one sample data set that

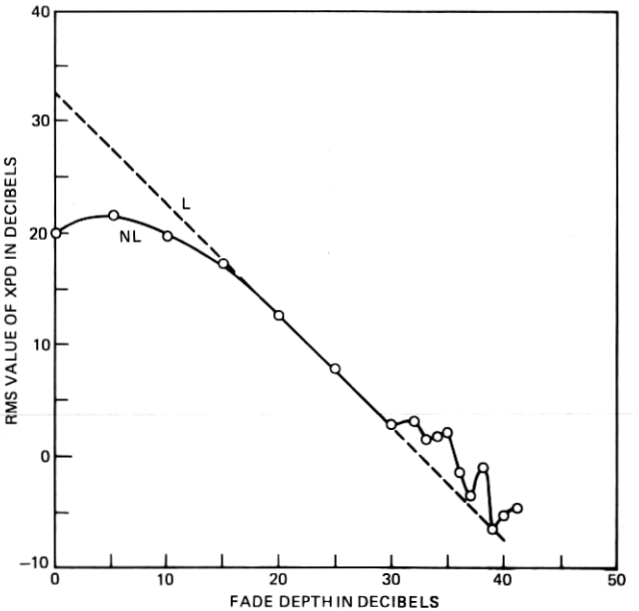

Fig. 1—RMS value of cross-polarized interference voltage as a function of fade depth. (Atlanta to Palmetto, Georgia, June 1974, 11 GHz.)

shows this type of behavior. A model for the cross-polarized signal that accounts for this observed behavior is proposed and developed in detail in this paper.

This proposed model for cross-polarized interference describes the signal as a sum of two components

$$V_{TX} = V_{DX} + V_{RX}, \tag{1}$$

where

V_{TX} = peak amplitude of the voltage envelope of the total signal received due to the transmitted cross-polarized signal.
V_{DX} = peak amplitude of the envelope of a "direct" received component, due to the transmitted cross-polarized signal.
V_{RX} = peak amplitude of the envelope of a random received component, due to the transmitted cross-polarized signal.

The component V_{DX} derives from imperfect polarization isolation in system hardware, and is subject to fading behavior identical to that of the copolarized signal. The random component V_{RX} is attributed to random spatial and temporal conditions that characterize the propagation path, and it is not subject to fading, thereby giving rise to the observed behavior of curve NL in Fig. 1. This random component is described here as a gaussian random process, which, as shown below, results

in V_{TX} becoming a Rice-Nakagami distributed random variable. This result is supported by experimental data taken at Palmetto, Georgia, as discussed by Lin.[4]

Use of a gaussian model for V_{RX} is based on the multiplicity of effects that can contribute to this component and on the conjecture that random scattering is a dominant mechanism. The generalized parametric modeling study of outage statistics carried out in this paper is predicated in part on this latter assumption. Without a model for the dependence of the random component of the interference signal on path length, outage-time estimates are limited to those few hop lengths where sufficient experimental data is available to specify the magnitude of this component.

In a companion paper in this issue, Lin[4] also uses the proposed Rice-Nakagami model for cross-polarized interference voltage to compute, by essentially the same method, estimates of DPF channel multipath outage time for QCPSK systems for two existing radio hops with and without space-diversity protection. To provide perspective on some of the principal differences between Lin's study and ours, the following comments are provided:

(*i*) Lin's analysis of experimental propagation data provides support for the Rice-Nakagami model for cross-polarized interference.

(*ii*) Estimates of outage time for two specific hop lengths are provided by Lin, whereas in this study hop length is a free model parameter. As a result, in Lin's study, outage time for intermediate hop lengths must be inferred through linear interpolation between the two point estimates. The physical conditions corresponding to such interpolated values are not clear, since the two (experimental radio path) interpolation end points correspond to different hardware and propagation path characteristics. Also, this linear interpolation, performed on semilog outage time plots, corresponds to a simple power law dependence of outage time on path length.

(*iii*) Some effects of space diversity on multipath outage time are considered in Ref. 4, but not here.

(iv) The sensitivity of multipath outage time to differences between theoretical and experimental DPF channel performance characteristics, and the implications for potential outage time reductions, are presented in this study, but not in Ref. 4.

II. DPF RADIO-CHANNEL PERFORMANCE DURING MULTIPATH FADES

2.1 Multipath-fading outage probability

During multipath fading, a DPF radio-channel outage occurs whenever the channel BER exceeds some defined threshold for acceptable service.

Two service outage thresholds are considered here: BER = 10^{-3} and BER = 10^{-6}. A service outage results if

(*i*) a multipath fade occurs and exceeds the thermal-noise fade margin (conventionally defined fade-margin), or

(*ii*) the polarization isolation (XPD) of the DPF-channel degrades below that necessary to maintain the required error rate (assuming both polarizations are in service).

The effect on outage time of spectral distortions due to the frequency selectivity of multipath fades is not considered here. As a result, optimistic estimates of multipath fading outages are obtained, and can be viewed as lower bounds for actual outage times.

Under the condition that multipath fading is present, the probability of a DPF digital-radio channel outage occurring as a result of a multipath fade on a single radio hop is given by the expression

$$P_{\text{OUT}} = \int_0^\infty P_e(\text{BER} \geqq \text{BER}_0|L)p_F(L)dL, \tag{2}$$

where $L \equiv$ peak envelope voltage normalized to the nominal (unfaded) value—i.e., the ratio of faded to unfaded peak amplitude of the voltage envelope, and where $P_e(\text{BER} \geqq \text{BER}_0|L)$ is the complement of the conditional probability distribution for the channel bit-error rate, (i.e., the probability that the BER of the channel exceeds that for acceptable service (BER_0), at a given fade level L), and the function $p_F(L)$ is the probability density function for the amplitude of the multipath fading signal.

The conditional probability P_e for exceeding a given bit-error rate BER_0, given a fixed fade level L, is defined by the relation

$$P_e(\text{BER} \geqq \text{BER}_0|L) = \begin{cases} \displaystyle\int_{V_M(L)}^\infty p_{VX}(\xi|L)d\xi & \text{for } L \geq L_m(D) \\ 1.0 & \text{for } L < L_m(D) \end{cases}, \tag{3}$$

where p_{VX} is the conditional density function for the cross-polarized interference-signal envelope, $V_M(L)$ is the maximum value of V_{TX} for which the desired BER_0 can be obtained with the channel signal faded to L, and $L_m(D)$ is the minimum-allowable normalized amplitude of the received-signal envelope for a path length D required to maintain some specified maximum channel BER_0—i.e., the fade level at the system thermal-noise threshold. [See Section 3.1 for a graphical interpretation and explanation of (3) and (4).]

It is instructive to rewrite (2) in the following form, using the definition in (3):

$$P_{OUT} = \int_0^{L_m(D)} p_F(L)dL + \int_{L_m(D)}^{\infty} \int_{V_m(L)}^{\infty} p_{VX}(\xi|L)p_F(L)d\xi dL. \tag{4}$$

The first term on the right-hand side of eq (4) represents the outage time resulting from fades below the system thermal-noise threshold $L_m(D)$, while the second term represents outage time resulting from degradation of cross-polarization isolation during fades down to the threshold $L_m(D)$.

To estimate total outage probability (or outage time), which results during multipath fades, statistical models are required for both the copolarized and cross-polarized signals as received on the copolarized receiving channel during multipath fading conditions. In the deep-fade region (fades in excess of 10 dB) an accepted statistical model for the peak envelope voltage of a signal is given by the probability distribution function,[1,8]

$$P_F(l \leqq L) = (1 - e^{-L^2}) \cong L^2. \tag{5}$$

This distribution function results in the density function

$$p_F(L) = \frac{d}{dl} P_F(l \leqq L) = 2Le^{-L^2} \cong 2L \tag{6}$$

required in the outage probability expression, eq (2).

It is shown below that restriction of the statistical model for the peak envelope voltage L to the deep-fade region does not restrict results of practical interest. This fortunate circumstance results because outage statistics accumulate almost entirely during time intervals that correspond to this deep-fade region.

With the proposed model for the cross-polarized interference voltage, it can easily be shown that the conditional probability density function of the envelope of the cross-polarized interference voltage at a fixed fade depth L is given by the expression[9]

$$p_{VX}(V|L) = \frac{V}{\sigma_{RX}^2} I_0 (C_0 LV/\sigma_{RX}^2) \exp\left(-\frac{V^2 + (C_0L)^2}{2\sigma_{RX}^2}\right), \tag{7}$$

where σ_{RX}^2 = variance of the gaussian component of the cross-polarized interference voltage, $I_0(\cdot)$ is the modified Bessel function of order zero, and $0 \leqq C_0 \leqq 1.0$ is (approximately) the ratio of the cross-polarized interference to copolarized envelope voltages received during unfaded propagation conditions, i.e.,

$$C_0 = 10^{-(XPD_0/20)},$$

where XPD_0 is the cross-polarization discrimination ratio with no multipath fading. (Voltages used here and in all subsequent expressions are

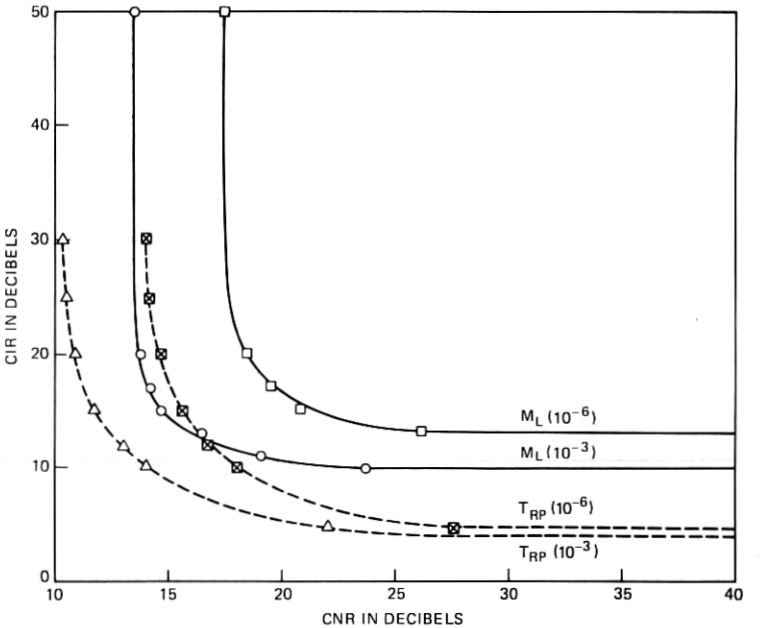

Fig. 2—DPF-channel digital radio performance curves plotted for constant bit-error rate.

given normalized to their unfaded levels.) Expression (7) is known as the Rice-Nakagami probability density function.[5–7]

2.2 Characterization of channel performance at constant bit-error rate

A graphical representation of the relation between carrier-to-interference ratio (CIR) and carrier-to-(thermal) noise ratio (CNR) at constant bit error rate for a DPF channel can be derived from recent theoretical studies.[10,11] The two dashed curves shown in Fig. 2 were obtained from results given in the above referenced works and represent the relationship between CIR and CNR at bit-error rates of 10^{-3} and 10^{-6}. For convenient reference, such curves are referred to as DPF-channel performance curves in this study.

For a single interferer (the cross-polarized interference signal of the DPF channel), the relation between V_{TX} and CIR is

$$\text{CIR} = 20 \log_{10}(V_c/V_{TX}). \tag{8a}$$

Note that, in terms of the normalized voltage $V_M(L)$, which appears in (3), the values of CIR that correspond to a DPF-channel performance curve are given by the expression

$$\text{CIR}_{\text{BER}_0} = -20 \{\log_{10}[V_M(L)]\}. \tag{8b}$$

The relationship of L to CNR is given by

$$\text{CNR}(D) = \text{CNR}_0(D) - \text{FD}(L), \tag{8c}$$

where $\text{CNR}_0(D)$ is the nominal unfaded design value of CNR for a path of length D, and

$$\text{FD}(L) = -20 \log_{10}(L) \tag{8d}$$

is the channel fade depth (L as defined above). The quantity $\text{CNR}_0(D)$ can also be expressed as

$$\text{CNR}_0(D) = \text{CNR}_{th} + \text{FM}(D), \tag{9}$$

where CNR_{th} is the thermal-noise threshold value of CNR for a given BER_0 with no interference present, and $\text{FM}(D)$ is the system thermal-noise fade margin for path length D.

The fade margin can be written as

$$\text{FM}(D) = -20 \log_{10}[L_m(D)], \tag{10}$$

where $L_m(D)$ is the normalized thermal-noise threshold signal level as previously defined.

The solid curves shown in Fig. 2 present data from laboratory measurements of 3A-RDS performance for 10^{-3} and 10^{-6} bit-error rates. Note that threshold values for CIR are apparent from this figure—i.e., a value CIR_0 below which a given BER is exceeded independent of CNR. Use of both theoretical and experimental channel performance curves in this modeling study is intended to provide some insight into those non-ideal channel performance factors that significantly influence multipath outage time. These comparisons are unique to this paper.

2.3 Multipath-fading outage time

Experimental results on multipath fading statistics at 11 GHz provide the basis for obtaining estimates of expected DPF radio-channel outage time. From these measurements the expression for multipath-caused outage time in minutes per year can be written as

$$T_{\text{OUT}} = rT_0P_{\text{OUT}}, \tag{11}$$

$$r = \text{multipath occurrence factor}$$

$$T_0 \equiv (t/50)\ 1.33 \times 10^5 \text{ minutes} \qquad 35° \leqq t \leqq 75°,$$

where t is average temperature in °F.

The variable T_0 represents the time period during which fading outages can accumulate (see Vigants[12]). The multipath occurrence factor r is a normalization coefficient required to account for the influence of climate, terrain, signal frequency, and path-length on the quantitative

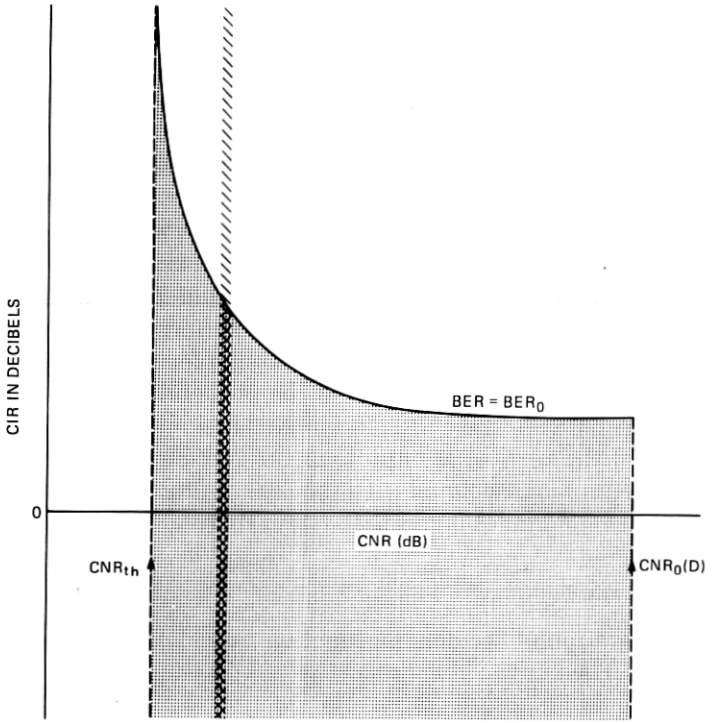

Fig. 3—Graphic representation of outage-probability computation.

statistical behavior of a signal during multipath fades—i.e., it is required to account for variations in the fraction of time that multipath occurs. This factor is defined by the expression.[1]

$$r = c(f/4)D^3 10^{-5}, \tag{12}$$

where

c = geographic factor accounting for terrain and humidity effects (typically $0.25 \leqq c \leqq 4$, with $c = 1.0$ for average terrain and climate).
f = frequency in GHz.
D = path length in miles.

III. OUTAGE ESTIMATES

3.1 Graphical interpretation

The expressions given in Section II for outage probability during multipath fading can be interpreted graphically in terms of a DPF channel performance curve. In the discussion that follows, refer to Fig. 3, which shows a hypothetical performance curve for some fixed BER_0.

Associated with each point in the plane defined by the CNR and CIR axes is a probability density for the occurrence, during multipath fading conditions, of that pair of values (CIR, CNR) that define this point. All points lying along a line perpendicular to the CNR axis correspond to a fixed fade depth (cross-hatched strip), while all those points lying below the performance curve correspond to the condition BER $\geqq$ BER_0 (shaded region).

In terms of Fig. 3, the expression for the probability P_e (BER $\geqq$ $BER_0|L$), eq. (3), represents the integration of the probability density of occurrence of all points along a line (fixed value L) perpendicular to the CNR axis and lying in the region below the performance curve (double cross-hatched portion of strip). The expression for total outage probability P_{OUT} is then the integration of the probabilities along all such strips between CNR_{th} and $CNR_0(D)$ (shaded region). The entire region to the left of the vertical asymptote of the DPF-channel performance curve (at CNR_{th}) is associated with the outage probability component which results from fades below the system thermal noise threshold.

3.2 Analytic results

The integration of the density function $p_{VX}(V|L)$ indicated in eq. (3) can be carried out to give the analytic expression

$$P_e(\text{BER} \geqq \text{BER}_0|L) = \begin{cases} \exp\left\{-\dfrac{\alpha^2(L)+\beta^2(L)}{2}\right\} & \\ \times \displaystyle\sum_{k=0}^{\infty} \dfrac{\left[\displaystyle\sum_{j=0}^{k}\left(\dfrac{\beta^2(L)}{2}\right)^j / j!\right]\alpha^{2k}(L)}{2^k k!} & ;\ \text{CNR} \geqq \text{CNR}_{th} \\ 1.0 & ;\text{CNR} < \text{CNR}_{th}, \end{cases} \tag{13}$$

where

$$\alpha(L) = \frac{C_0 L}{\sigma_{RX}} \tag{14}$$

$$\beta(L) = \frac{V_M(L)}{\sigma_{RX}}. \tag{15}$$

For convenience in computations, a DPF-channel performance curve is represented analytically by the expression

$$\text{CIR}(D) = K_1 \text{Log}_{10}[1.0 - 10^{-K_2|(\text{CNR}-\text{CNR}_{th})/K_3-\text{CNR})|}] + \text{CIR}_0, \tag{16}$$

Table I — Empirical DPF-channel performance curve parameters

Curve	K_1	K_2	K_3	CNR_{th}	CIR_0
T_{RP} BER = 10^{-3}	−12.90	1.00	35.0	10.25	4.1
M_L BER = 10^{-3}	−7.55	1.09	30.0	13.399	9.95
T_{RP} BER = 10^{6}	−13.79	0.95	35.0	13.85	4.85
M_L BER = 10^{6}	−8.70	0.85	30.0	17.3998	12.9

T_{RP} signifies DPF-channel performance characteristics derived from theoretical results given by Rosenbaum[10] and Prabhu.[11]

M_L signifies DPF-channel performance characteristics derived from laboratory measurements on 3A-RDS.

where K_1, K_2, and K_3 are fitting parameters determined empirically to approximate closely the data points as shown in Fig. 2. Table I gives sets of values for the various parameters in eq. 16 used to approximate the performance curves required for subsequent calculations.

Table I also establishes the notation that denotes the DPF-channel performance curve used to obtain specific results: T_{RP} denotes use of the DPF-channel performance curves derived from results obtained by Rosenbaum[10] and Prabhu;[11] M_L denotes use of the DPF-channel performance curves derived from 3A-RDS laboratory measurements.

Table II presents other expressions and parameter values used in subsequent calculations.

3.3 Propagation path and system hardware effects

From the previous expressions for outage probability (eq. 2, and eqs. 11 through 15), it is apparent that outage time statistics for a DPF-channel are dependent on the parameters D (hop length), C_0 (equipment polarization isolation), σ_{RX} (propagation path phenomena), and r (multipath occurrence factor).

Measures of the sensitivity of DPF-channel outage statistics to system hardware characteristics (as represented by C_0) and to propagation path characteristics (as represented by σ_{RX}) are important for evaluating system design and cost.

Table II — Definitions and parameter values pertinent to numerical calculations

Parameter	Definition
Section loss (SL)	SL = 27.0 + 20.0 $\log_{10}$ (D) where D is in miles
System gain (SG)	SG = FM + SL, where FM ≡ fade margin
SG for BER ≦ 10^{-6}	$SG_{10^{-6}}$ = 108 dB
SG for BER ≦ 10^{-3}	$SG_{10^{-3}}$ = 112 dB

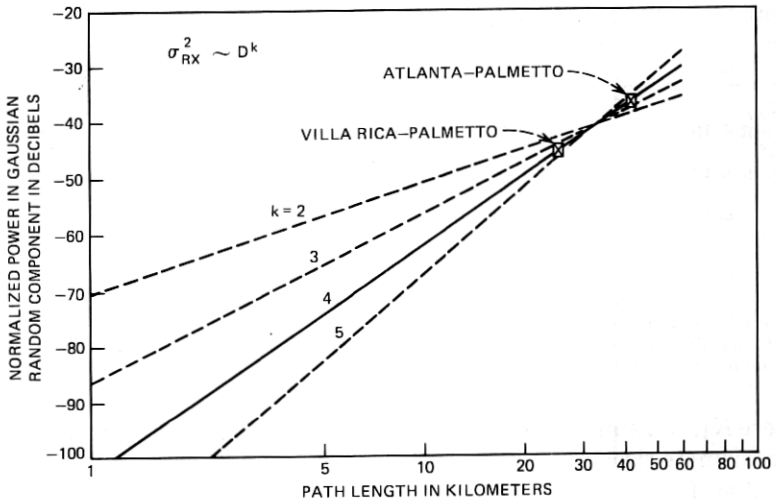

Fig. 4—RMS value of random component of cross-polarized interference voltage as a function of path length: power law approximations to experimental data points.

3.3.1 Propagation-path scattering hypothesis

The parameter σ^2_{RX}, a measure of the energy in the random component of the cross-polarized signal, is probably dependent on a variety of propagation-path parameters. At present, this conjectured path dependence is not clearly understood theoretically, nor is sufficient experimental data available to establish an empirical model. Experimental measurements[4] at Palmetto Ga., taken on two propagation paths, provide the only directly applicable data for σ^2_{RX}. These two data points are shown plotted in Fig. 4, along with various power law relationships between σ^2_{RX} and distance D.

To compute outage statistics via the expressions for P_{OUT} [eq. (2)], a functional dependence of σ^2_{RX} on path length D is required. Using the two available data points, we find that an approximate path-length power-law dependence of D^4 would provide a reasonable fit (12 dB per double distance). However, this rate of increase in energy of the random cross-polarized signal component seems too large from the standpoint of physical intuition to apply over any substantial path length interval.

Based on the hypothesis that terrain scattering is a primary contributor to the energy in V_{RX}, a very simple, idealized, theoretical estimate of σ^2_{RX} as a function of path length D was obtained for three antenna tower heights (see Appendix B). Figure 5 summarizes results of these estimates scaled to the experimental value for σ^2_{RX} obtained on the longer of the two propagation paths at Palmetto (26.4 mi/42.5 km). This empirical scaling of the estimate for σ^2_{RX} is equivalent to use of a scattering

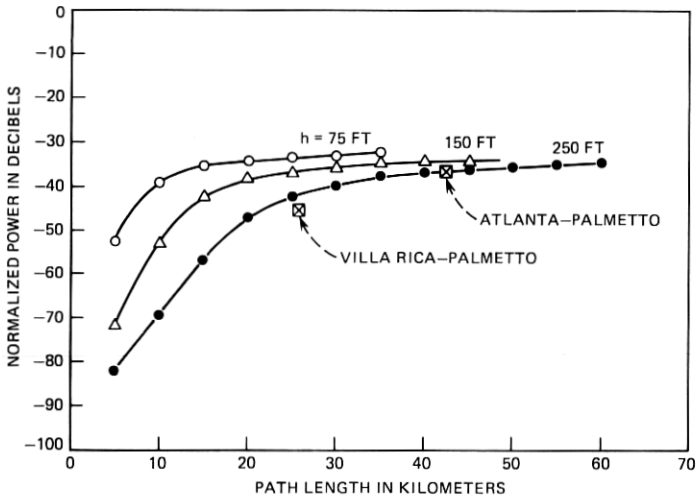

Fig. 5—Prediction for power in random component of cross-polarized interference signal based on terrain-scattering model.

cross section of about −28 dB, in general agreement with experimental data from radar terrain-backscatter measurements.[14,15] Note that while this scaling also produces reasonable agreement between these predictions and the measured value of σ_{RX}^2 on the shorter path at Palmetto, the different antennas, widely different antenna heights, and uneven terrain characterizing this latter path prohibit any detailed comparison.

In the absence of experimental data for other path lengths, and in view of the general agreement between the terrain scattering estimates and the Palmetto data points shown in Fig. 5, theoretical estimates of σ_{RX}^2 are used here to define a functional relation between this parameter and the path length D for a fixed tower height. The curve in Fig. 5 for the tower height $h = 250$ ft will be used for this purpose as a baseline in calculating outage statistics.

3.3.2 System hardware XPD requirements

Variations in P_{OUT}, which result from changes in the value of the parameter C_0, provide a measure of the sensitivity of a DPF radio channel to the level of polarization isolation (XPD) in the radio and antenna system hardware. For the two bit-error rates used here, Figs. 6 and 7 summarize calculations of channel outage statistics as a function of radio path length for several values of C_0 spanning a range of practical concern.

Two reference curves, "A" and "B," are shown in Fig. 6 and on all subsequent figures. Curve "A" represents the multipath fading outage time for a conventional single-polarization radio channel with identical

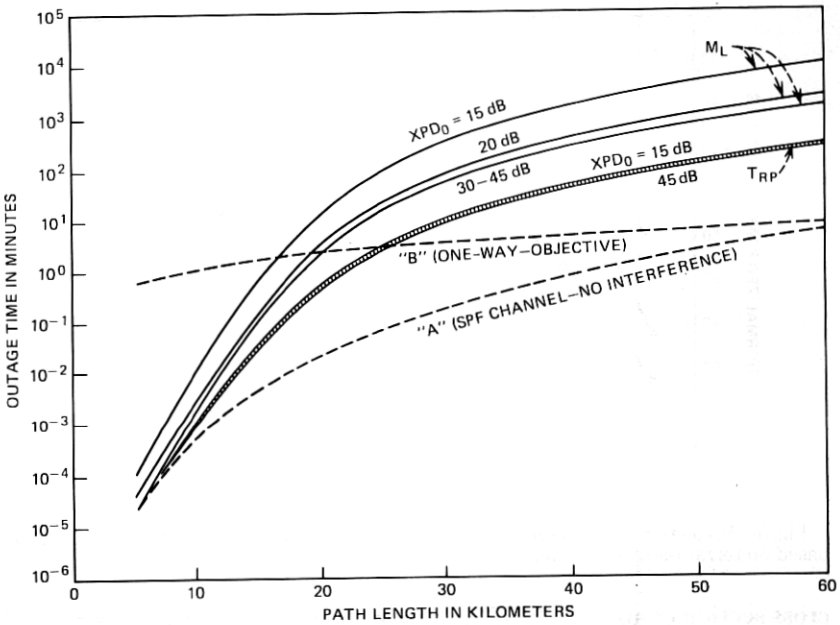

Fig. 6—Outage-time statistics as a function of hardware XPD for $BER_0 = 10^{-6}$.

thermal-noise fade margin and no interference, and curve "B" a per-hop one-way outage-time objective typical of that used in the design of short-haul radio systems. Reference curve "A" allows for comparisons to show the increase in outage probability suffered by a DPF radio channel over a conventional channel as a result of fade-dependent degradation in cross-polarization discrimination.

Outage-objective reference curve "B" shows, by its intersection with a DPF-channel outage curve, an upper limit on radio-path hop length at a given BER_0. This limit on path length is termed a maximum-reliable-path-length (MRPL) and is used here to illustrate implications of outage-time variations. The limit actually imposed on hop length for a DPF channel in practice must be determined by the combined outage probabilities resulting from rain, equipment failures, and multipath fading.[16]

These calculations indicate that for current DPF-channel performance characteristics, channel outage during multipath fading is quite insensitive to the polarization isolation of system hardware as long as a minimum isolation of 20 dB is maintained, i.e., $XPD_0 \geq 20$ dB. This lower bound, to an acceptable range for hardware XPD, can be extended to 15 dB in theory (see T_{RP} curves in Figs. 6 and 7), and can also be extended in practice for the larger bit-error-rate criterion ($BER_0 \leqq 10^{-3}$). However, for the measured DPF-channel performance curve at $BER_0 = 10^{-6}$, a

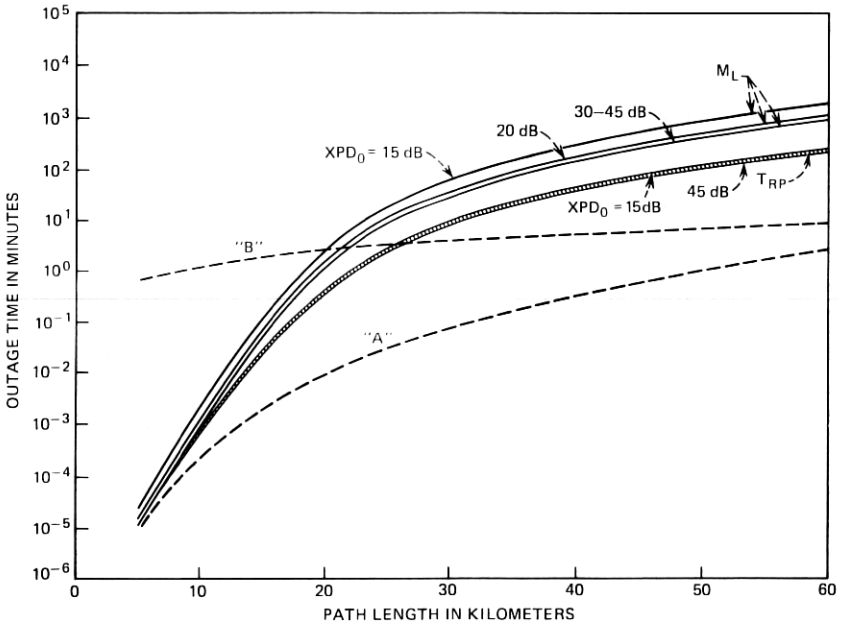

Fig. 7—Outage-time statistics as a function of hardware XPD for $BER_0 = 10^{-3}$.

system hardware $XPD_0 = 15$ dB degrades outage performance by almost an order of magnitude at any particular path length, and decreases the intercept of this outage curve and the one-way-objective curve "B" by 15 to 20 percent.

These results have significance from two standpoints. First, the XPD requirements on system hardware are moderate and are therefore less costly to implement. This is particularly important for the radio antenna system. Secondly, maintenance requirements for XPD characteristics are relatively loose, again producing a positive cost factor from an operational standpoint.

3.4 Numerical results: estimates of outage statistics

As discussed in Section 3.3.2, the outage probability is not sensitive to changes in the value of the parameter C_0. Consequently, all computations are performed for the upper and lower limits on the practical range of interest for C_0, i.e., $20 \text{ dB} \leqq 20 \log_{10}(C_0^{-1}) \leqq 45 \text{ dB}$. Since these computed results bracket those for all intermediate values of C_0, a strip or band of values is shown, in general, rather than a single curve in the graphical results presented below. Note that in some cases this "band" has, effectively, zero width and appears to be only a single curve.

The simple relationship between the outage time (T_{OUT}) and outage probability (P_{OUT}) for a single radio hop during multipath fading is given

by eq (11) in Section 2.3. All results given below for T_{OUT} are computed according to eq. (11) with an average temperature of $t = 55°F$, which gives a value of $T_0 = 1.467 \times 10^5$ minutes.

Note that all results obtained below are for an "average" multipath environment corresponding to the value $c = 1.0$ in the expression (12) for the multipath occurrence factor. All results can be applied directly to other environments by direct scaling of outage time via a simple multiplication by the appropriate value of c.

3.4.1 Deep-fade restriction on statistical model

Figures 8 and 9 show representative sets of curves that display the dependence of outage probability on the faded signal level L. The curves in Fig. 8 represent the integrand in the expression for P_{OUT} (eq. 2), and are computed for constant path length D, for the value $XPD_0 = 20$ dB. From these curves, it is apparent that with adequate hardware XPD ($XPD_0 \geqq 20$ dB), significant contributions to P_{OUT} occur only for fades $L \leqq 0.32$ ($-20 \log_{10}(L) \geqq 10$ dB). This result supports the adequacy of the statistical model for the signal envelope peak value used here in calculating outage statistics for a DPF channel.

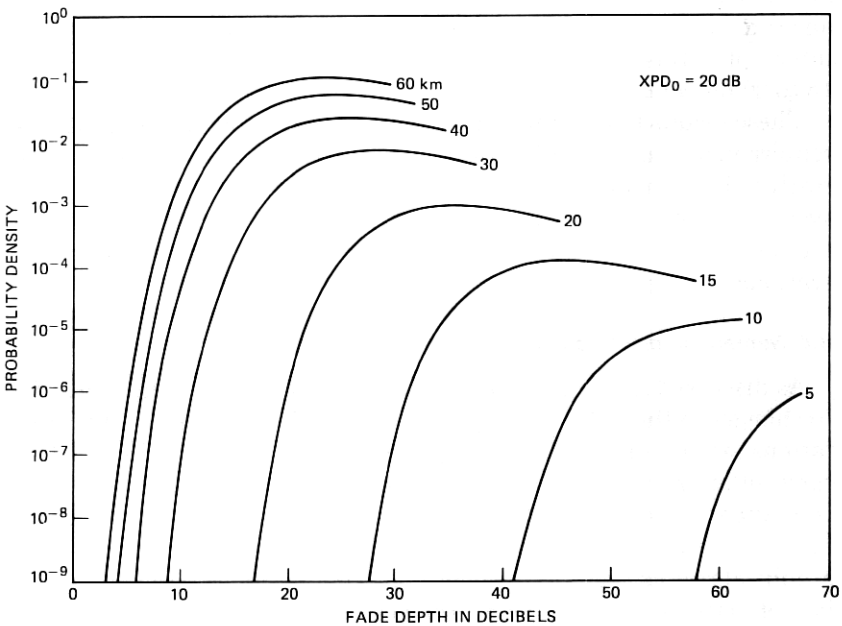

Fig. 8—Functional dependence of $\{P_e(\text{BER} \geqq 10^{-6}|L)\, p_F(L)\}$ on fade depth $[-20 \log_{10}(L)]$ for M_L channel characteristics.

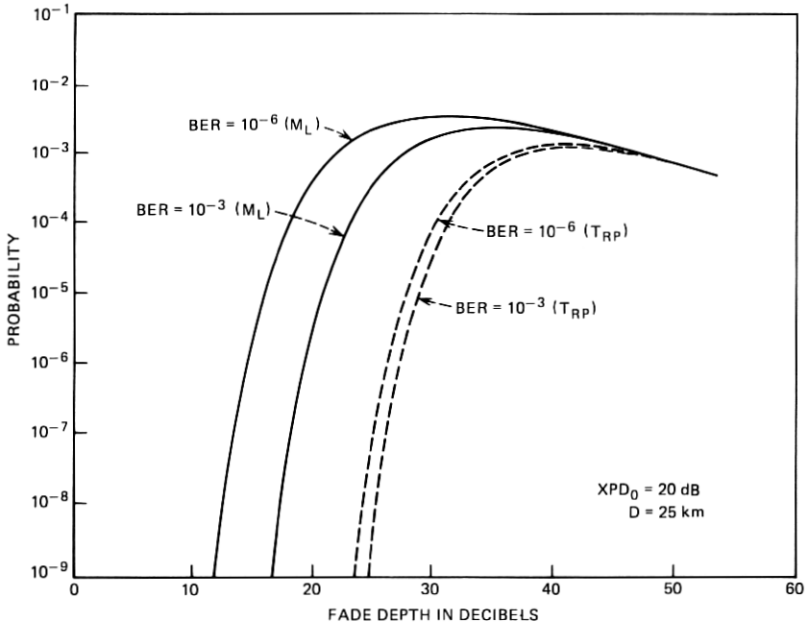

Fig. 9—Functional dependence of $[P_e(\text{BER} \geqq \text{BER}_0|L)\ p_F(L)]$ on fade depth $[-20 \log_{10}(L)]$ for M_L and T_{RP} channel-performance curves.

3.4.2 Path-length dependence of T_{OUT}

Figure 10 summarizes results obtained by computing outage time for average terrain and climate conditions ($c = 1.0$ in eq. 12) on a single hop for a DPF channel. Curves are presented for two bit-error rates: $\text{BER}_0 = 10^{-6}$ and $\text{BER}_0\ 10^{-3}$.

Comparison of the curves computed using theoretical and measured DPF-channel performance curves show the effect of degradations introduced by intersymbol interference and other non-ideal conditions in the digital terminal and associated radio equipment. Most important in this respect is the threshold value CIR_0, which appears to dominate other parameters.

From Figure 10, it is apparent that for the model parameters used here the error-rate criterion used to specify an MRPL (or, for a particular path length of interest, the expected outage time) is not critical. Theoretically, the change in MRPL that results in going from 10^{-3} BER to 10^{-6} BER is less than 5 percent, while for results based on measured DPF-channel performance, the change is only about 10 percent.

At a particular path length, the increase in outage time incurred by going from 10^{-3} to 10^{-6} BER is at most a factor of 2 for results based on either the theoretical or measured DPF-channel performance curves.

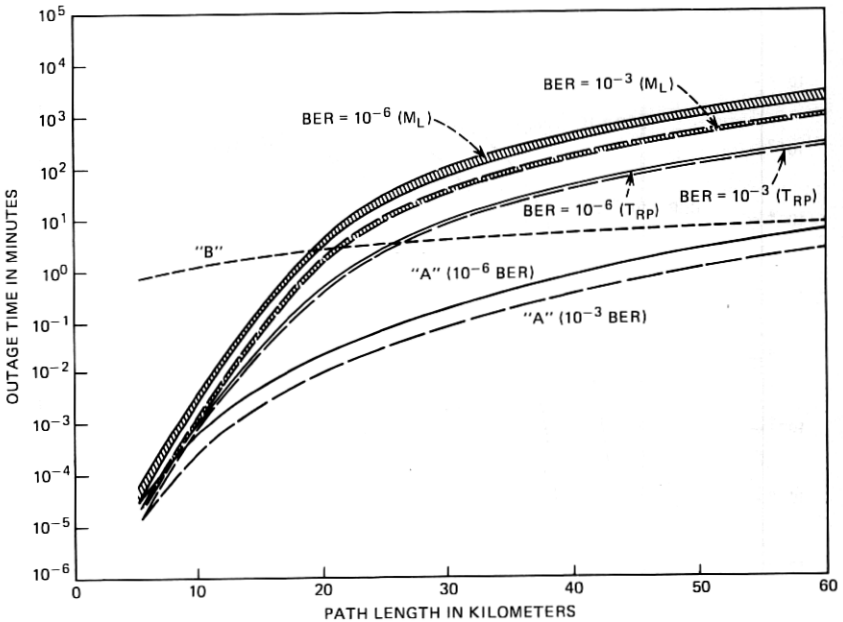

Fig. 10—Outage time vs path length for T_{RP} and M_L channel-performance curves.

The outage time estimates obtained for measured DPF-channel performance result in a net decrease of about 20 to 25 percent in MRPL from those estimates obtained using theoretical performance.

Figure 11 draws a comparison between outage-time estimates obtained under the terrain-scattering hypothesis for two different antenna tower heights for $BER_0 = 10^{-6}$. The difference in the estimated outage time for these two cases decreases with increasing path length, varying from about three orders of magnitude at 10 km to about a factor of 5 at 35 km.

The MRPL decreases by about 60 percent in going from the 250-ft tower to the 75-ft tower, indicating a large increase in cross-polarized energy contributed by terrain scattering (see Fig. 5). Assuming that the terrain-scattering model is valid (or at least dominant), this result suggests that use of large tower heights would be desirable for DPF-channel radio systems.

3.4.3 Dependence of T_{OUT} on system gain

An index of performance for a radio system is the quantity known as system-gain (SG). System gain is defined as the required difference between transmitted and received signal-power levels necessary to achieve some standard level of performance. As above, the two performance standards considered here are $BER_0 = 10^{-3}$ and $BER_0 = 10^{-6}$. Typical

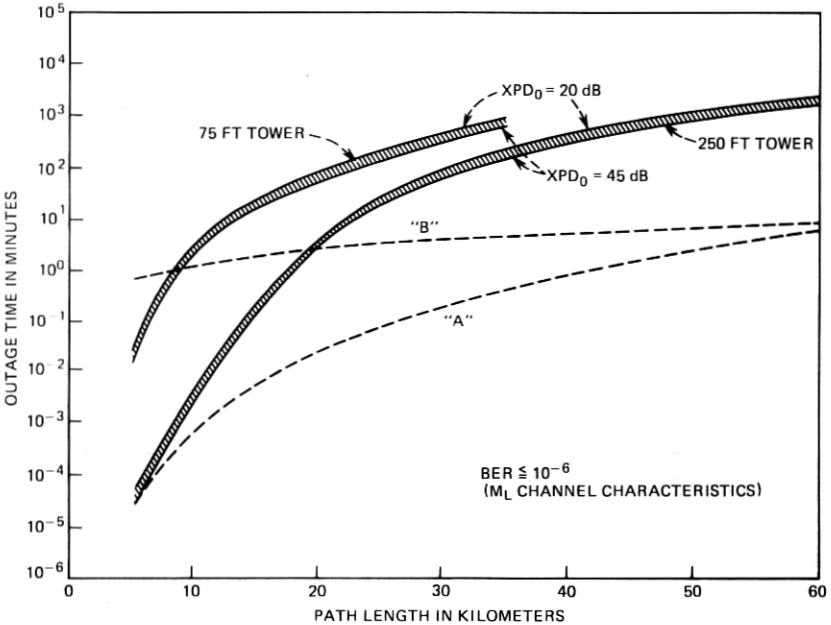

Fig. 11—Outage-time statistics for two antenna tower heights under terrain-scattering hypothesis.

system-gain values for commercially available DPF-channel digital radio systems vary from 95 to 108 dB for a bit-error rate limit of 10^{-6}.

To evaluate the effect of system gain on outage time statistics, calculations of T_{OUT} have been made using SG as a parameter (with XPD_0 = 20 dB). Figures 12 and 13 summarize results obtained for the two bit-error rate standards, with SG varying from 95 to 115 dB in 5 dB steps.

Results for the two different error rates are quite similar. Based on theoretical DPF channel performance, outage-time statistics vary somewhat (less than a factor of 2) as the system gain increases from 95 to 100 dB, but remain virtually unchanged in the range $100 \leqq SG \leqq 115$ dB.

Using measured DPF-channel performance for the model parameters used here, outage time is almost totally insensitive to system gain for path lengths in excess of 18 to 20 km. For shorter path lengths, some differences in outage time do result as system gain is changed, but since the values of outage time for these short paths are very small in comparison to the system objective, such variations are not of practical concern.

For path lengths in the vicinity of the MRPL, system gain does not appear to affect significantly the outage performance of a DPF channel.

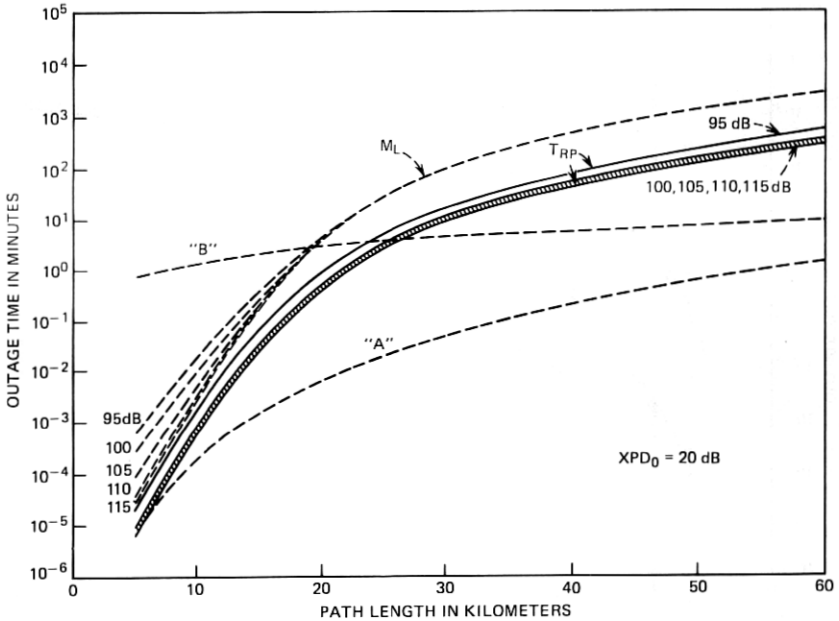

Fig. 12—Outage-time statistics as a function of system gain for DPF radio channel with $BER_0 = 10^{-6}$.

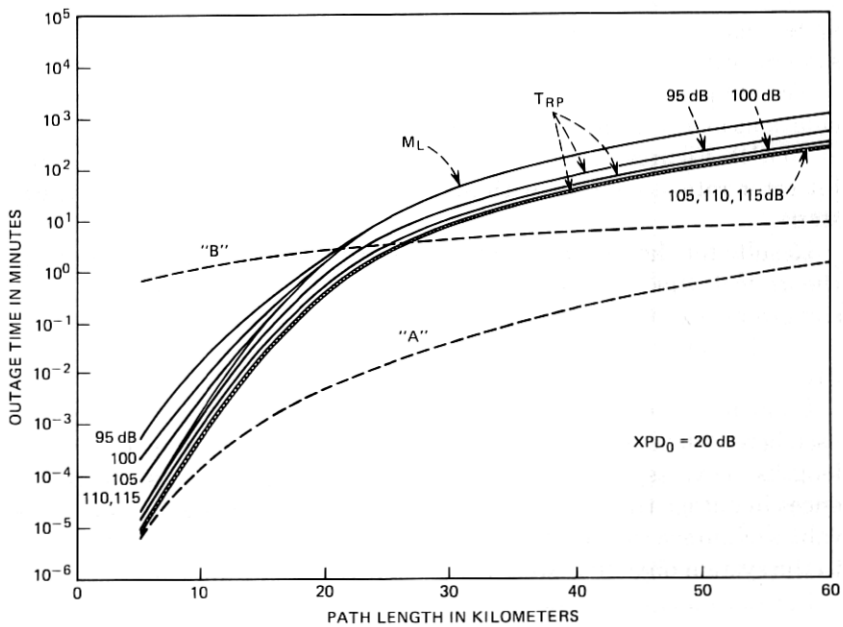

Fig. 13—Outage-time statistics as a function of system gain for a DPF channel with $BER_0 = 10^{-3}$.

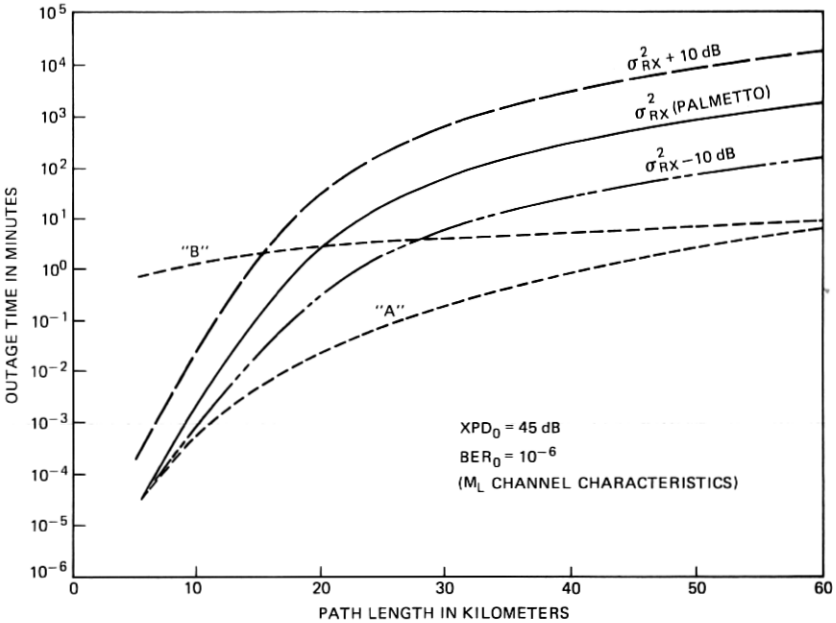

Fig. 14—Sensitivity of outage-time statistics to power level of random component of cross-polarized signal.

3.4.4 Environmental sensitivity of T_{OUT}

As discussed in Section 3.3.1, outage statistics are dependent on propagation path characteristics expressed through the parameter σ^2_{RX}. Various characteristics of the geographic location of a radio propagation path will influence the value of σ^2_{RX}. To explore the sensitivity of results obtained here to change in the magnitude of σ^2_{RX}, calculations for T_{OUT} were carried out with σ^2_{RX} as a parameter.

Figure 14 summarizes results obtained by computing T_{OUT} as a function of path length for three values of σ^2_{RX}; in each case, σ^2_{RX} has the same relative variation with D—e.g., the curve shown in Fig. 5 for h = 250 ft. These computations show that T_{OUT} varies by about one order of magnitude as σ^2_{RX} varies by one order of magnitude (10 dB). (The midrange value of σ^2_{RX} corresponds to that obtained from the Atlanta-to-Palmetto, Georgia data set at 42.5 km.)

These results indicate the importance of obtaining data on σ^2_{RX} from a variety of locations to establish its range of variability. Depending on the magnitude of such variations, the allowable path length for reliable digital communication via DPF radio-channels could vary significantly with geographic location—e.g., the results shown in Fig. 14 show potential changes of ±25 to ±30 percent as σ^2_{RX} varies by ±10 dB.

IV. SUMMARY

4.1 Radio-system XPD requirements

An important consideration for the practical implementation of DPF digital radio systems is the degree of isolation required between the two orthogonal, linearly polarized waves transmitted at each frequency. Severe requirements on such isolation (XPD) imply increased system costs resulting both from hardware design and system maintenance.

In general, a minimum requirement of 20 to 25 dB for hardware XPD is not severe from either a design or maintenance standpoint. This level of XPD results in DPF channel error-rate performance well above the minimum service standards used here for unfaded signals (see Fig. 2).

The estimates of outage statistics obtained in this study with a variety of model parameters indicate that outage performance for current DPF channels during multipath fading is not materially affected by the system-hardware XPD as long as it remains better than 20 dB (see Figs. 6, 7, and 10). Multipath-related outages do not, therefore, impose any severe hardware design or maintenance requirements.

4.2 Maximum reliable path length

The example outage estimates computed in the above sections for representative system parameter values suggest that for a 0.02 percent two-way reliability objective for a 400-km route, and with a high antenna tower (250 feet), the maximum reliable path length (MRPL) for a DPF channel is about 21.5 km (13.4 mi) for a bit-error rate of 10^{-3} in the absence of other outage effects, *and for an average multipath environment* (see Fig. 10). This MRPL can vary from 17.5 km (10.9 mi), on Gulf Coast or overwater paths, to 31.0 km (19.3 mi) in dry, mountainous regions (Albuquerque), reflecting changes in the magnitude of the multipath occurrence factor for these environmental extremes.

For a bit-error rate BER $\leqq 10^{-6}$, the range of MRPL in these example calculations is 17.0 km (10.6 mi) to 26.0 km (16.2 mi) with a value of 20.0 km (12.4 mi) *for an average multipath environment.*

The rather steep slope of an outage-time curve of Fig. 10 in the vicinity of its intersection with the outage-time objective curve "B" indicates that the changes in MPRL resulting from inclusion of rain and equipment outages will not be severe, i.e., a small decrease in MRPL allows for a substantial contribution to outage time from these other sources of channel outage. Note that the preceding statement does not hold for rain-limited propagation paths (e.g., in the Miami, Florida area) where multipath outages are strongly dominated by rain-induced outages. The actual magnitude of such changes will, however, depend on the rain statistics for a given geographic location.

4.3 Dependence of path length on system gain

For digital radio systems with high system gain, the exact value of system gain, while significant for the average BER performance of a DPF channel, does not significantly affect the MRPL. In the examples considered here, changes on the order of 20 percent in system gain (in dB) result in very small changes in MRPL—i.e., less than 1.0 km.

4.4 General conclusions

The model proposed and developed here for DPF-channel outages during multipath fading, together with results obtained from the example calculations carried out for representative system and environmental parameter values, lead to the following general conclusions:

(*i*) Outage times during multipath fading conditions are between two and three orders of magnitude larger for a DPF channel of current design than for a conventional (single-polarization-per-frequency) radio channel with no interference.

(*ii*) The threshold carrier-to-interference ratio (CIR_0) below which a given bit-error rate cannot be obtained, independent of the signal-to-noise (thermal) ratio, is the channel performance characteristic of greatest importance to multipath outages. Up to an order of magnitude improvement in outage time could be obtained if a near theoretical value of CIR_0 could be achieved through hardware/design improvements.

(*iii*) Multipath outage time is dependent on geographic and environmental conditions expressed through the multipath occurrence factor r and the statistical parameter σ_{RX}^2. Outage-time estimates computed here scale almost linearly with changes in σ_{RX}^2, other model parameters remaining approximately constant.

(*iv*) Under the hypothesis that terrain scattering is the dominant mechanism for the random component of the interference signal in a DPF channel, multipath outage time for such channels can be minimized through use of high antenna towers and, when possible, through judicious choice of radio-hop terrain.

V. ACKNOWLEGMENTS

The author is indebted to A. J. Giger for suggesting this study of multipath outages in dual-polarized digital radio channels and to the following individuals for various helpful technical discussions: W. T. Barnett, G. L. Frazer, A. J. Giger, S. H. Lin, and T. L. Osborne. The author is also indebted to Mr. Osborne for his encouragement and help in publishing this study.

APPENDIX A

Symbol Table

$\alpha(L) = C_0 L/\sigma_{RX}$.
$\beta(L) = V_M(L)/\sigma_{RX}$.
σ_{RX} = Standard deviation of random component of cross-polarized signal.
σ_N = Normalized, cross-polarizing, bistatic, terrain-scattering cross section.
BER = Bit-error rate.
BER_0 = Fixed maximum value for BER.
c = Geographic multipath-fading normalization factor.
C_0 = Ratio of cross-polarized to copolarized signal voltages during periods of no multipath fading—i.e., $C_0 = 10^{-(\text{XPD}_0/20)}$.
CIR = Carrier-to-interference ratio in dB for single interferer arising from cross-polarized DPF-channel signal.
CNR = Carrier-to-(thermal)-noise ratio in dB.
CNR_0 = Nominal unfaded design value of CNR.
CIR_0 = Value of CIR below which BER_0 is exceeded independent of CNR.
CNR_{th} = thermal-noise threshold value of CNR at a given BER_0 with no interference present.
D = Path length (miles or kilometers).
f = Frequency in GHz.
FD = Channel fade depth $[-20 \log_{10}(L)]$.
FM = System thermal-noise fade margin.
h = Tower height for radio antennas.
I_0 = Modified Bessel function of order zero.
$\{K_1, K_2, K_3\}$ = Empirical fitting parameters for DPF-channel performance curves.
L = Ratio of faded to unfaded peak envelope voltage.
L_m = Minimum allowable normalized amplitude of the received-signal envelope (for a path length D) required to maintain some specified maximum channel BER_0.
MRPL = Maximum-reliable-path-length. (The path length determined by the intersection of an outage time curve and the system outage-time-objective curve).
M_L = DPF-channel performance characteristics derived from laboratory measurements on 3A-RDS.
P_e = Conditional probability of DPF-channel BER exceeding some specified value BER_0 at a given, fixed multipath fade level L.
$p_F(L)$ = Probability density function of multipath fading signal.

P_F = Probability distribution function of multipath fading signal.
P_{out} = Probability of DPF-channel BER exceeding some specified value BER_0 during periods of multipath fading.
P_r = Receiving antenna radiation pattern.
P_t = Transmitting antenna radiation pattern.
p_{VX} = Conditional probability density of cross-polarized interference envelope voltage.
r = Multipath occurrence factor.
R_1 = Distance from transmitting antenna to terrain-scatter point.
R_2 = Distance from terrain-scatter point to receiving antenna.
SG = System-gain (the difference between transmitted and received signal power levels necessary to achieve some standard level of performance, i.e., BER = BER_0).
t = Average temperature in °F.
T_0 = Base time period for multipath fading activity during one year.
T_{out} = Total time (in minutes per year) during which the DPF-channel BER can be expected to exceed some BER_0 as a result of multipath fading activity.
T_{RP} = DPF-channel performance characteristics derived from theoretical results given by Rosenbaum[10] and Prabhu.[11]
V = Peak envelope voltage.
V_M = Maximum normalized value of V_{TX} for which BER $\leqq$ BER_0.
$\langle v_{RS}^2 \rangle$ = Energy received as a result of terrain scattering, including conversion from one linear polarization to the orthogonal linear polarization.
V_{DX} = Peak envelope voltage of direct component of cross-polarized signal.
V_{RX} = Peak envelope voltage of random component of cross-polarized signal.
V_c = Peak envelope voltage of copolarized signal.
V_{TX} = Peak envelope voltage of total cross-polarized signal.
XPD = Cross-polarization-discrimination ratio (ratio of copolarized to cross-polarized received signal in dB).
XPD_0 = Cross-polarization discrimination ratio during period of no multipath fading.

APPENDIX B

B.1 Estimation of σ_{RX}^2 Based on Terrain-Scattering Hypothesis

Terrain scattering along the radio-hop propagation path is one physical phenomenon that can contribute energy to the random component of the cross-polarized interference signal in a DPF radio channel.

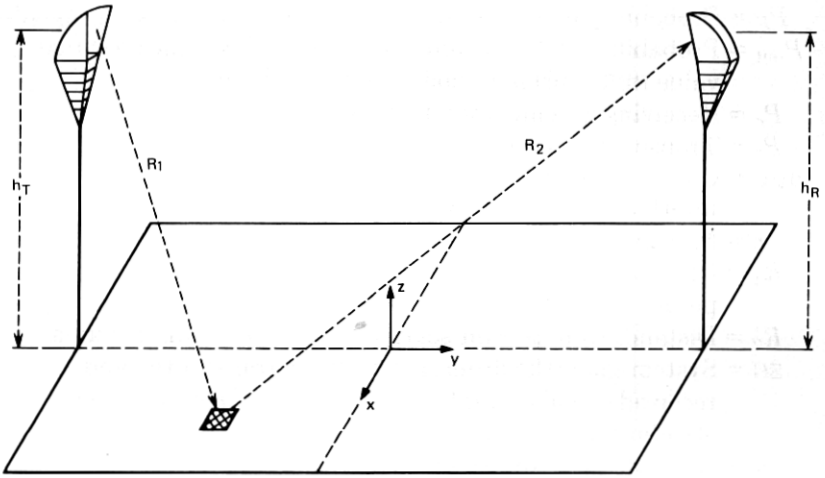

Fig. 15—Idealized radio-hop geometry used in terrain-scattering computation.

The magnitude of this component is not easily determined experimentally or theoretically, but an estimate can be obtained through an idealized numerical calculation scaled to available data.

Figure 15 shows the geometry assumed as a basis for calculating the energy contributed to the cross-polarized-interference signal by terrain scattering. The expression used to compute this random-scatter component is

$$\langle v_{RS}^2 \rangle = \int\int dxdy \left\{ \sigma_N(x,y) \frac{P_t(x,y)}{R_1^2} \frac{P_r(x,y)}{R_2^2} \right\}, \tag{17}$$

where $\sigma_N(x,y)$ is a factor proportional to the cross-polarized, bistatic scattering cross section of the ground and various normalization factors. Interest here is centered on the functional dependence of $\langle v_{RS}^2 \rangle$ on radio-hop path length, rather than the absolute magnitude of this quantity. The functions P_t and P_r are the antenna response patterns at the transmitter and receiver, respectively.

Given this restricted interest and the very sharply directive radiation pattern of typical transmitting and receiving antennas at 11 GHz (a pyramidal horn-reflector-antenna response pattern was used for calculations performed here), the variation of $\sigma_N(x,y)$ with location is neglected and assumed to have unity value. The area over which the double integration shown in eq. (17) is performed is limited by an error criterion for the incremental contributions that occur during evaluation of this expression. The error criterion used corresponds to neglecting contributions from areas illuminated by very low-level side-lobes of the transmitting antenna radiation pattern, and sensed by the low-level side-lobe region of the receiving antenna response pattern.

Normalizing the computed estimates to the experimental values obtained at Palmetto, Georgia (see Section 3.3.1), the normalized scattering cross section has a value of about −28 dB, which agrees within a few dB with radar cross-section measurements on various types of terrain.[14,15]

The results of the calculations of scattered cross-polarized energy are summarized in Fig. 5 for three different tower heights. These curves display an approximate path-length dependence varying from D^2 for long paths to D^6 for short paths.

REFERENCES

1. W. T. Barnett, "Multipath Propagation at 4, 6, and 11 GHz," B.S.T.J., *51,* No. 2 (February 1972), pp. 321–361.
2. W. T. Barnett, "Determination of Cross-Polarization Discrimination During Rain and Multipath Fading at 4 GHz," IEEE 1974 International Conference on Communications, June 17–19, 1974, Minneapolis, Minnesota, Conference Record, pp. 12D-1–12D-4, IEEE Cat. No. 74, CHO 859-9-CSCB.
3. G. LeFrancois, L. Martin, and M. Rooryck, "Influence of the Propagation on the Value of the Decoupling of Two Orthogonal Polarizations," Ann. Telecommun., 28 (1973) pp. 316–324.
4. S. H. Lin, "Impact of Microwave Depolarization During Multipath Fading on Digital Radio Performance," B.S.T.J., this issue, pp. 645–674.
5. S. O. Rice, "Mathematical Analyses of Random Noise," B.S.T.J., *23,* No. 3 (July 1944), pp. 282–332, and *24,* No. 1 (January 1945), pp. 46–256.
6. M. Nakagami, "The M-Distribution—A General Formula of Intensity Distribution of Rapid Fading," in W. C. Hoffman (Ed.), *Statistical Methods in Radio Wave Propagation,* Oxford: Pergaman, 1960.
7. P. Beckmann, *Probability in Communication Engineering,* New York: Harcourt, Brace and World, 1967.
8. S. H. Lin, "Statistical Behavior of a Fading Signal," B.S.T.J., *50,* No. 10 (December 1971), pp 3211–3270.
9. W. B. Davenport and W. L. Root, *An Introduction to the Theory of Random Signals and Noise,* New York: McGraw-Hill, 1968, pp. 165–166.
10. A. S. Rosenbaum, "PSK Error Performance with Gaussian Noise and Interference," B.S.T.J., *48,* No. 2 (February 1969), pp. 413–442.
11. V. K. Prabhu, "Error Rate Considerations for Coherent Phase-Shift Keyed Systems with Co-Channel Interference," B.S.T.J., 48, No. 3 (March 1969), pp. 743–767.
12. A. Vigants, "Space Diversity Engineering," B.S.T.J., *54,* No. 1 (January 1975), pp. 103–142.
13. K. A. Norton, L. E. Vogler, W. V. Mansfield, and P. J. Short, "The Probability Distribution of the Amplitude of a Constant Vector Plus a Rayleigh Distributed Vector," Proc. IRE, *43* (October 1955), pp. 1354–1361.
14. M. W. Long, *Radar Reflectivity of Land and Sea,* Lexington Books, Lexington, Mass.: D. C. Heath, 1975.
15. C. R. Grant and B. S. Yaplee, "Back Scattering from Water and Land at Centimeter and Millimeter Wavelengths," Proc. IRE (London), *47,* No. 7 (July 1957), pp. 976–982.
16. M. S. Levetin, "A New Approach to Setting Reliability Objectives for Microwave Radio Systems," IEEE International Conference on Communications, June 14–16, 1976, Philadelphia, Pa.